Surface effects on the electrodiffusion of alkali-metal ions and protons in quartz

J. Plata, J. Breton, E. Alvira, and V. Delgado
Departamento de Física Fundamental y Experimental, Universidad de La Laguna, 38203 Tenerife, Spain

C. Girardet*
Laboratoire de Physique Moléculaire, Université de Besançon, La Bouloie, 25030 Besançon CEDEX, France
(Received 4 May 1990)

The influence of the surface on the electromigration of alkali-metal ions or protons acting as charge compensators of trivalent impurity centers in quartz is determined on the basis of potential surface calculations. Proton compensator migration depends on the ability for proton penetration at the anode interface. The ionic current density depends on the ability for alkali-metal ions to escape at the cathode interface. A study of the potential energy experienced by the diffusive ion during its migration through the quartz surface and onto the surface plane allows us to determine the diffusion path and to calculate the jump frequencies of the surface potential for Li^+, Na^+, and H^+. The penetration and escape processes are shown to be preponderant for the evaluation of the ionic current density in the electromigration mechanism.

I. INTRODUCTION

In α-quartz, impurity ions such as Al, Ge, Fe, B, and Ti are known to lie in Si substitutional sites and to be associated each with a nearby interstitial proton or monovalent alkali-metal ion that provides electric charge compensation for the whole defect.[1] These defects are responsible for deleterious effects (frequency change and reduction in quality factor) of quartz resonators and they have been extensively studied by various experimental probes.[2] Sweeping quartz with an electric field of 20–2000 V cm^{-1} and at $T \simeq 750$ K is a well-established empirical method for improving the resonator performance.[3]

The microscopic interpretation of electrodiffusion of alkali-metal ions is, however, a somewhat complicated problem that requires an undersanding of the following physical process questions.

(i) How does the ion migration proceed inside the bulk quartz sample and what is the phenomenon implied in the charge compensation effect?

(ii) How does the sample surface influence the alkali-metal ion or proton diffusion mechanism both at the anode and cathode?

(iii) Where, and in what way, are the alkali-metal ion and proton neutralized by electrons at the cathode?

In recent papers,[4–7] we have examined the bulk electrodiffusion of alkali-metal ions M^+ (M=Li,Na,K) and protons (H^+) located inside optical channels of a β-quartz sample with infinite dimensions [item (i), no surface effect]. The potential surface experienced by M^+ or H^+ has been first determined[4] in the neighborhood of the impurity trivalent center (Al^{3+}) and far from this center. The dynamics of M^+ has then been described[5] within the transit-time-concept approach (mass-dependent-rate theory), and the behavior with time of the ionic current density has been calculated for various temperatures of the sample. The substitution mechanism of M^+ ions by protons has also been studied[6,7] within the so-called diffusion-compensation model in order to interpret the time variation of the ionic current at short and long times.

In these diffusion models, the surface influence was disregarded for simplicity, though its inclusion appeared to us as fundamental in a quantitative estimate of the ionic current intensity. The goal of this paper is to account for this influence in the M^+ (H^+) migration mechanism and to model the ion penetration and escape. Section II is devoted to the presentation of the microscopic scheme defining the sweeping. The method used to describe the structure of the quartz surface and the potential energy experienced by M^+ or H^+ is presented in Sec. III. Numerical calculations for M^+ or H^+ superficial migration on the quartz surface and for the ion penetration into the sample are given in Sec. IV and the results are discussed in Sec. V.

II. MICROSCOPIC SCHEME OF THE ELECTRODIFFUSION

A. General

The sweeping of a quartz sample in ambient atmosphere is schematized in Fig. 1. The Pt foils are in macroscopic contact with the quartz sample. The external electric field is switched on at time $t=0$.

At $t<0$, alkali-metal ions (M^+) are assumed to be exact charge compensators of trivalent centers randomly distributed in the sample. The protons, which will act as new compensators when the M^+ ions are swept, are either located in the bulk quartz or outside the sample.

At $t>0$, the diffusion of the bulk protons will not be influenced by the surface, while the outer protons, which will diffuse inside the quartz channels, must first penetrate the surface. We assume that these outer protons are initially located at the interface between the

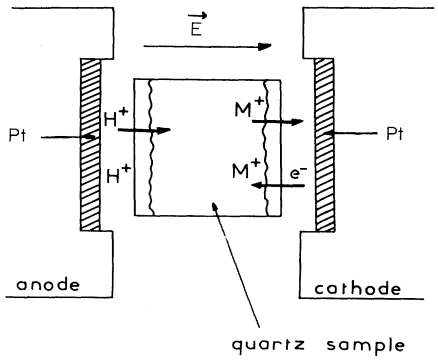

FIG. 1. Quartz sweeping principle. Two Pt foils are intercalated between the electrodes and the quartz sample.

anode Pt foil and the quartz solid.

A microscopic study of the penetration mechanism of protons inside the solid requires a definition of the Pt-quartz interface, which itself depends on the mechanical and chemical treatments of the quartz surface. This surface is assumed to be planar, cut perpendicular to the optical axis of the crystal, and formed predominantly by oxygen atoms. This latter hypothesis is consistent with the results of a statistical study[8] on the atomic distribution at the quartz surface. Moreover, a HF chemical treatment at the surface leads to the occurrence of the OH bonds. The distribution and orientation of these bonds are not known and we make the additional ansatz that they form a regular overlayer with OH orientations along the direction of the oxygen-ghost Si atoms due to the cut. The surface layer is then schematized as a regular arrangement of Si and O ions with an unreconstructed structure. The O ions are H terminated, thus forming a thin slab of oriented electric dipoles.

At the anode side, an outer proton or alkali-metal ion located at the position $\mathbf{r}$ with respect to the surface origin experiences the potential

$$V_{\mathrm{H}}(\mathbf{r})=V_{\mathrm{H}}^{B}(\mathbf{r},\xi)+V_{\mathrm{H}}^{S}(\mathbf{r})+V_{\mathrm{H}}^{\mathrm{Pt}}(|D-z|)+e\mathcal{E}z \ . \quad (1)$$

The first term in Eq. (1) characterizes the potential due to the bulk quartz crystal, including the lattice distortion ξ and the influence of the trivalent centers. The second and third terms describe the interface influence, i.e., the effect of the quartz surface (OH bonds) and the effect of the metal surface; the interface is assumed to be formed by two planar parallel surfaces at a distance D. The latter term in Eq. (1) corresponds to the external electric field.

At the cathode side, two different, and simultaneous, phenomena can take place: (i) the alkali-metal ions remain inside the quartz sample and are electrically neutralized by electrons emerging from the Pt foil; (ii) the alkali-metal ions escape from quartz and are deposited onto the Pt foil. Experiments[9] show that the two processes coexist since quartz becomes smoky when submitted to a radiation field [item (i)] and alkali-metal deposition is observed on the Pt foil after sweeping [item (ii)].

Process (i) corresponds to an electron tunneling from the metal to the cation slab in quartz, with an effective work function that can be lowered with respect to the mean value of 5.5 eV for a free planar Pt surface, due to the nature of the interface. In contrast, process (ii) characterizes the direct escape of alkali-metal ions in the cathode interface and their capture by the metal surface. Each M^+ ion must then jump the potential barrier defined by the quartz surface, including the influence of the Pt foil.

The potential energy experienced by M^+ or H^+ in their motion at the cathode is expressed as

$$V_M(\mathbf{r}')=V_M^B(\mathbf{r}',\xi')+V_M^s(\mathbf{r}')+V_M^{\mathrm{Pt}}(|D+z'|)+e\mathcal{E}z' \ . \quad (2)$$

This equation is written in a symmetrical form with Eq. (1); the first and second terms characterize the influence of the bulk and surface quartz sample. including the distortion ξ', whereas the third and fourth terms are connected to the Pt foil and external electric field influences. r' describes the position of the M^+ ion with respect to the quartz surface.

B. Penetration and escape diffusion mechanism

We disregard here the bulk electromigration of ions, which has been considered elsewhere,[5–7] and focus on the penetration dynamics of H^+ or M^+ in quartz. To be consistent with the description of the bulk migration, we use a transport theory based on a steady-state approach.[5,10] The ion transport is modeled as a random-walk process and the diffusion constant is directly correlated to the transit time of M^+ (or H^+) in a given potential well. The jump frequency above a potential barrier V_n is defined as[10]

$$k_n=\left[\frac{k_BT}{2\pi\mu^*}\right]^{1/2}\frac{\exp(-V_n/k_BT)}{\int_{R_{n-1}}^{R_n}dr\,\exp[-V(r)/k_BT]} \ , \quad (3)$$

where k_BT is the Boltzmann energy and μ^* defines the effective mass of the ion, which can differ from the real mass due to the momentum transfer of M^+ (H^+) to the surrounding particles. The integral of the potential given by Eqs. (1) or (2) over the reaction (diffusion) coordinate r is restricted to the path between two consecutive maxima R_{n-1} and R_n of $V(r)$. The computation of the jump frequency requires a detailed knowledge of the potential function $V(r)$ and more particularly of the successive minima and maxima of this function outside and inside the quartz sample.

Equation (3) also holds for the superficial migration of the alkali-metal ions and protons onto the quartz surface (without penetration), which is another possible process for the ion motions. It could also apply to the escape dynamics of M^+ or H^+ ions out to the quartz at the cathode side.

Note that this transit-time theory is limited to the description of single jumps from one well to the closest well, and it cannot describe high-energy processes for the M^+ (H^+) dynamics. These latter processes, which would account for the multiwell jumps, are nevertheless very unprobable for the actual physical conditions of quartz sweeping.

III. THE POTENTIAL FUNCTION

A. System geometry

Although the experimental temperature for electromigration ($T \simeq 750$ K) corresponds to the α variety for quartz, we have chosen the simpler geometry of β-quartz. The differences of bond angles and distances between the two species are sufficiently small[11] to assume that the electromigration mechanism will not be affected by this change. β-quartz crystallizes in the hexagonal structure D_6^4 ($P6_222$) with lattice parameters $a=4.99$ Å and $c=5.456$ Å.

The sample contains randomly distributed trivalent centers of aluminum, only; the center that is closer to the surface than all the others has the main influence on the alkali-metal ion or proton dynamics. Its position inside the optical channel of quartz can be varied with respect to the surface.

As mentioned in Sec. II, the quartz surface is planar, with regularly arranged OH groups at the outer surface plane. The orientations of the OH bonds are those of the O—Si bonds. Moreover, the Pt foils (Fig. 1) are schematized as ideal conductors with perfect planar surfaces. The interfaces are thus formed by vacuum slabs with parallel surfaces containing protons or alkali-metal ions ($M \equiv$ Li or Na); their thickness is D.

The M^+ (H^+) ion has the running position $\mathbf{r}$; the diffusion (reaction) coordinate is not rectilinear and we thus choose the z axis as being collinear to the axis of an optical channel inside quartz.[4] The origin $z=0$ is taken as the intersect of the surface plane and of the $\mathbf{z}$ axis.

B. Potentials

The various terms in Eq. (1) [or in equivalent way, Eq. (2)] are now defined. The interaction between the ion (M^+ or H^+) at a position $\mathbf{r}$ inside or outside the bulk crystal is given as[4–6]

$$V^B(\mathbf{r},\xi)=\sum_{m,n,p}{}^{*}\,[v_{M,\text{H-Si}}(\mathbf{r},\xi)+\sum_{q}{}^{*}\,v_{M,\text{H-O}}(\mathbf{r},\xi)] + v_{M,\text{H-Al}}(\mathbf{r},\xi^0)\ , \tag{4}$$

where the indices m,n,p are integers that determine the positions of the silicon atoms, except for the Al-substituted atom, and the q index ($q=2,4$) characterizes the oxygen atoms associated with the corresponding (m,n,p)th Si. The first oxygen shell, not included in this sum, will be considered later [Eq. (6)]. The latter term corresponds to the interaction between the M^+ (H^+) ion and the Al^{3+}-impurity center. The distortions ξ and ξ^0 occur as the result of the presence of the Al center and of the M^+ (H^+) ion. Each term in Eq. (4) defines a pairwise potential that characterizes the electrostatic, induction, dispersion, and repulsion contributions, according to the relation

$$v_{ij}=\frac{q_iq_j}{r_{ij}}-\tfrac{1}{2}[\alpha_i\mathbf{E}_{ij}^2(r_{ij})+\alpha_j\mathbf{E}_{ij}^2(r_{ij})] -4\varepsilon_{ij}\left[\frac{\sigma_{ij}}{r_{ij}}\right]^6\left[1-\left[\frac{\sigma_{ij}}{r_{ij}}\right]^6\right]\ . \tag{5}$$

TABLE I. Potential parameters.

	q/e[a]	α (Å^3)	σ (Å)	ε (eV)
Si	0.4	6.81	1.8	0.275
O	−0.2	0.72	2.1	0.012
Al-H^+	0			
Al-Li^+	0.1	11.0	2.0	0.160
Al-Na^+	0.1			
OH[b]	0	0.72	2.31	0.005
H^+	0.4			
Li^+	0.3	0.03	0.70	2.980
Na^+	0.5	0.24	1.50	0.920

[a]Effective charges obeying the charge neutrality condition, reduced by the electronic charge. For the Al atom these charges are different depending on the second impurity (proton and various alkali-metal ions) (cf. Refs. 4 and 6).
[b]The OH superficial group has the oxygen polarizability and effective Lennard-Jones parameters calculated from the usual combination rules.

$\mathbf{E}_{ij}$ defines the electrical field experienced by the ith atom and due to the jth atom. The effective charges q, the polarizabilities α, and Lennard-Jones parameters (ε,σ) for each atomic species are given in Table I. Their values have been determined in such a way that they reproduce the experimental barrier heights of the (Al-M^+) and (Al-OH)$^-$ centers.[4,6] Note that $\alpha=0$ for the proton, and the attractive dispersion term thus vanishes in that case. Moreover, the effective charges of the alkali-metal ions and of the proton are different inside and outside the crystal. For instance, in quartz, $q_H=0.4e$, while in the interace this charge is equal to unity.

The interaction between the ion (M^+ or H^+) and the quartz surface can be separated into two terms as

$$V^s(\mathbf{r},\xi)=\sum_{m,n,q}[v_{M,\text{H-OH}}(\mathbf{r},\xi)+v_{M,\text{H-dipole}}(\mathbf{r})]\ . \tag{6}$$

The first contribution characterizes the sum over the first oxygen layer ($p=0$) of the pairwise potential between the ion and the OH groups in the surface region [Eq. (5) and Table I]. The second contribution takes into account of the dipolar nature of the OH bonds ($\mu_{mnq}\simeq 1.5$ D), as

$$v_{M,\text{H-dipole}}=q_{M,\text{H}}\mu_{mnq}\frac{(\mathbf{r}-\mathbf{r}_{mnq})}{(|\mathbf{r}-\mathbf{r}_{mnq}|)^3}\ , \tag{7}$$

where the position of the (m,n,q)th surface dipole moment is defined as $r_{mnq}(p=0)$.[4] Note that the magnitude of this latter potential depends strongly on the orientational disorder of the dipoles by thermal agitation, and it can considerably decrease at high temperature due to the competition between the Pt-metal effect, the bulk crystal, and the external electric fields.

The influence of the perfectly conducting Pt foil on the ion (M^+ or H^+) is described by the image potential which nicely reproduces the charge-metal interaction within the jellium approximation for the metal:[12]

$$V_{M,H}^{Pt} \simeq -\frac{q_{M,H}^2}{2(|z-D|-z_0)}(1-e^{-\lambda(|z-D|-z_0)}) . \quad (8)$$

This form is valid when the ion-Pt surface distance is larger than the adjustable parameter $z_0=1.38$ Å. This statement is assumed to be verified in our case ($|z-D| \geq 2$ Å). The screening parameter λ is equal to 2.23 Å^{-1}.[12] Note that Eq. (8) depends on the value of the effective charge $q_{M,H}$, which, as already mentioned for Eq. (5), is different inside and outside the quartz crystal.

The latter contribution to the potential energy experienced by the M^+ (or H^+) ion corresponds to the effect of the electric field. The screening of this field in the crystal with respect to vacuum is once again contained in the reduced effective charge of M^+ (H^+). Equations (4)–(8) are then used to compute the interaction potential [Eqs. (1) or (2)] and the corresponding jump frequency [Eq. (3)] for Li and Na ions and for the proton.

IV. NUMERICAL RESULTS AND DISCUSSION

A. Numerical backgrounds

The potential surfaces experienced by M^+ or H^+ have been calculated by disregarding the dipolar influence of the superficial OH bonds and the image potential of Pt. These two contributions are discussed separately since both μ_{OH} and the interface thickness D are not known and they are considered as free parameters. The potential $V(x,y,z,\xi)$ is calculated when M^+ and H^+ are located in successive planes parallel to the surface with a path equal to $\Delta z = c/24 \simeq 0.225$ Å. Inside each plane we explore 784 points in a rectangle centered on the optical channel axis and defined by the coordinates of its tops $(\pm a/2, \pm\sqrt{3}a/2)$. We then determine the diffusion path as the curve joining the absolute minima of the potential calculated for the various planes. The curve defined by the points **r** which satisfy this minimum-energy require-

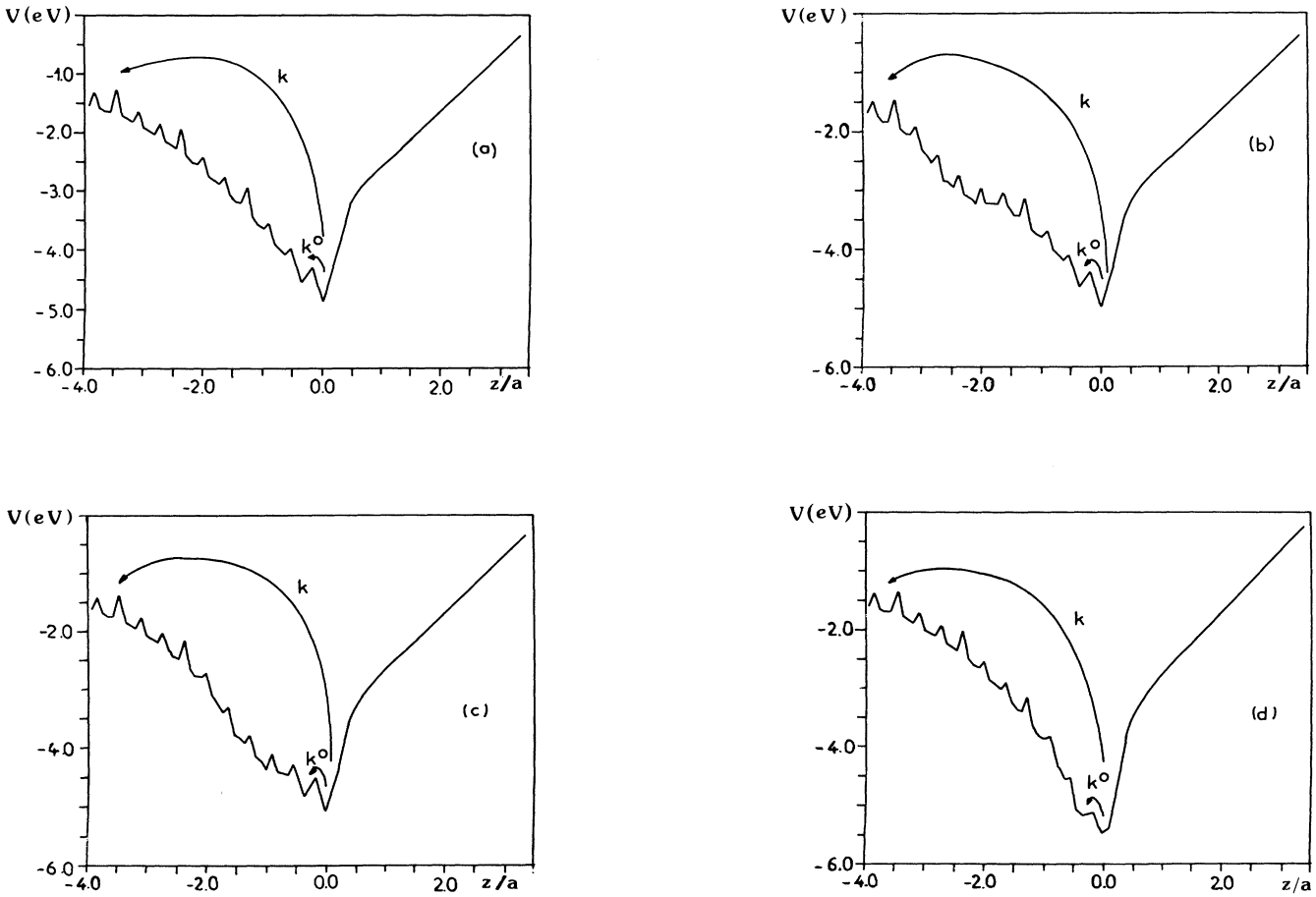

FIG. 2. Potential curves for the Li^+ diffusion through the quartz surface. The negative and positive values of z correspond to ion positions inside or outside the sample, respectively. The Al center is located at (a) $z=-\infty$, (b) $z=-11.82$ Å, (c) $z=-6.36$ Å, and (d) $z=-0.91$ Å. k^0 and k are the jump frequencies connected to the superficial penetration of the ion and to the bulk penetration, respectively.

ment characterizes the penetration potential. For the $z=0$ plane, the superficial diffusion coordinate is the curve $y(x)$ that connects the absolute minima when y is constant.

The distance z between the M^+ (H^+) ion and the quartz surface varies from negative values, inside the quartz crystal, to positive values, outside the crystal (i.e., inside the interface). When $z \leq -4c$ ($\simeq -22.48$ Å), the sum of Eq. (4) is over the crystal atoms (Si and O) located inside a sphere of radius $4c$ centered on the M^+ ion. This sphere, which satisfies the electric charge neutrality condition, ensures the convergence of the total potential with an accuracy better than 10^{-3} eV. In the range $-4c \leq z \leq 0$, the radius of the sphere still centered on the M^+ (H^+) ion is increased in order to include the same number of crystal atoms. When $z \geq 0$ we consider a half-sphere centered at the origin (0,0,0) filled with the same number of atoms, which satisfies, once again, the requirement of charge neutrality.

The potential surface and thus the M^+ dynamics for the surface penetration and diffusion depend on the position of the Al centers in the sample. Four situations have been considered. (a) The Al impurity is far enough from the surface to disregard its influence, this corresponds to a nearly perfect channel; (b) the Al center is located at $m_0=1$, $n_0=0$, and $p_0=-6$, i.e., at a distance of about 12 Å inside the crystal; (c) then the distance between the surface and the Al center is decreased to 6.4 Å ($m_0=1$, $n_0=0$, and $p_0=-3$); and finally (d) the Al center is located in the first Si plane ($m_0=1$, $n_0=0$, $p_0=0$) at a distance 0.9 Å from the OH layer.

In a second stage, the influence of the dipolar field due to the OH bonds adsorbed on the quartz and of the metal foil is introduced. The potential $V_{M,\text{H-dipole}}$ [Eq. (7)] is determined for an ideal orientation of the dipoles.[13] When the influence of the electric fields due to the metal and to the quartz surfaces is disregarded, the dipoles μ_{OH} are oriented along the broken O—Si bonds and the angle $(\mu_{OH}, \mathbf{n})$ is equal to 55° ($\mathbf{n}$ is the normal to the quartz surface). The calculation of the potential $V^{Pt}_{M,H}$ [Eq. (8)] is carried out for an interface thickness that is varied from $D=4$ Å to $D=20$ Å. The surface defects and corrugation are disregarded.

B. Ion penetration results

Figures 2(a)–2(d) exhibit the curve of potential minima experienced by Li^+ as a function of the distance with respect to the surface, in the case $V_{\text{dipole}}=V^{Pt}=0$ and for the four selected distances between the quartz surface and the closer Al center. When the Li^+ ion is outside the

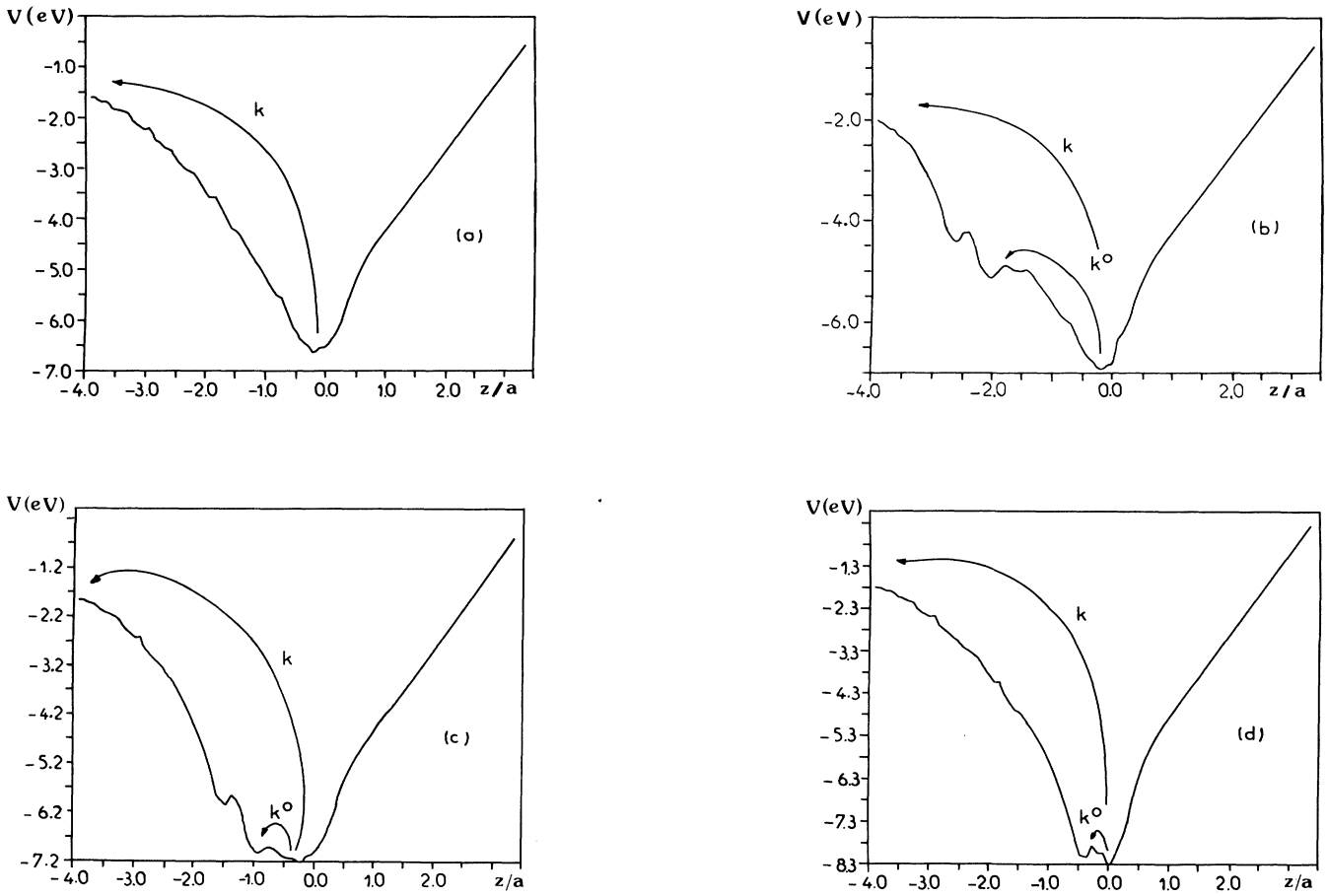

FIG.3. Potential curves for the Na^+ diffusion through the quartz surface; same as Fig. 2.

crystal, the potential monotonically decreases. At a distance from the surface equal to 2.5 Å, Li^+ experiences short-range dispersion-repulsion interactions due to OH terminations, and the slope of the potential curve increases up to the point where the ion reaches the quartz surface $z=0$. The shape of the potential depends on the position of the aluminum center. In a perfect channel, this potential exhibits a set of maxima and minima separated by a distance of about $c/3$, which corresponds to the distance between successive silicon and oxygen planes, with alternate positive and negative charges. When the Al center is drawn nearer to the surface, the overall shape of the inside potential is modified [Figs. 2(b)–2(d)] due to the increasing influence of the charge defect on the alkali-metal ion. The absolute potential minimum is obtained on the surface in all cases, but its depth increases as the Al center becomes closer to the crystal surface.

Similar potential curves are drawn for Na^+ in Figs. 3(a)–3(d). In contrast with the Li^+ penetration potential, the structure with potential minima and maxima does not occur in the perfect channel. For the channel with an Al center, this latter impurity strongly modifies the potential shape and depth as it is drawn nearer to the surface. The absolute minimum is not found on the crystal surface but slightly inside the sample ($z=-0.9$ Å) when the Al center lies far from or close to the surface [Figs. 2(a)–2(c)], or slightly outside the sample ($z=0.5$ Å) when Al is located on this surface.

TABLE II. Potential depths ΔV^0 and ΔV (eV) for the surface penetration and jump frequencies k^0 and k (s^{-1}) at $T=750$ K. [The four situations *a*, *b*, *c*, and *d* correspond to the various positions of the Al center in the channel (Figs. 2–4).]

Ion		ΔV^0	k^0	ΔV	k
Li^+	*a*	0.6	1.8×10^{9}	3.3	2.0×10^{-11}
	b	0.6	2.1×10^{9}	3.3	5.1×10^{-11}
	c	0.5	2.7×10^{9}	3.3	4.0×10^{-12}
	d	0.3	2.3×10^{9}	3.9	1.8×10^{-15}
Na^+	*a*			5	4.0×10^{-18}
	b	1.7	2.0×10^{-1}	4.9	6.4×10^{-21}
	c	0.3	1.3×10^{10}	5.5	2.2×10^{-24}
	d	0.4	4.5×10^{9}	6.5	2.0×10^{-31}
H^+	*a*			4.7	1.3×10^{-19}
	b	2.5	5.7×10^{-5}	4.5	8.6×10^{-19}
	c	1.1	2.3×10^{5}	4.9	1.3×10^{-20}
	d			5.7	1.4×10^{-26}

Figures 4(a)–4(d) are relative to the proton penetration potential that exhibits the same overall behavior as for Na^+ (no structure) and an absolute minimum, like Li^+, on the surface. We give in Table II, two characteristic

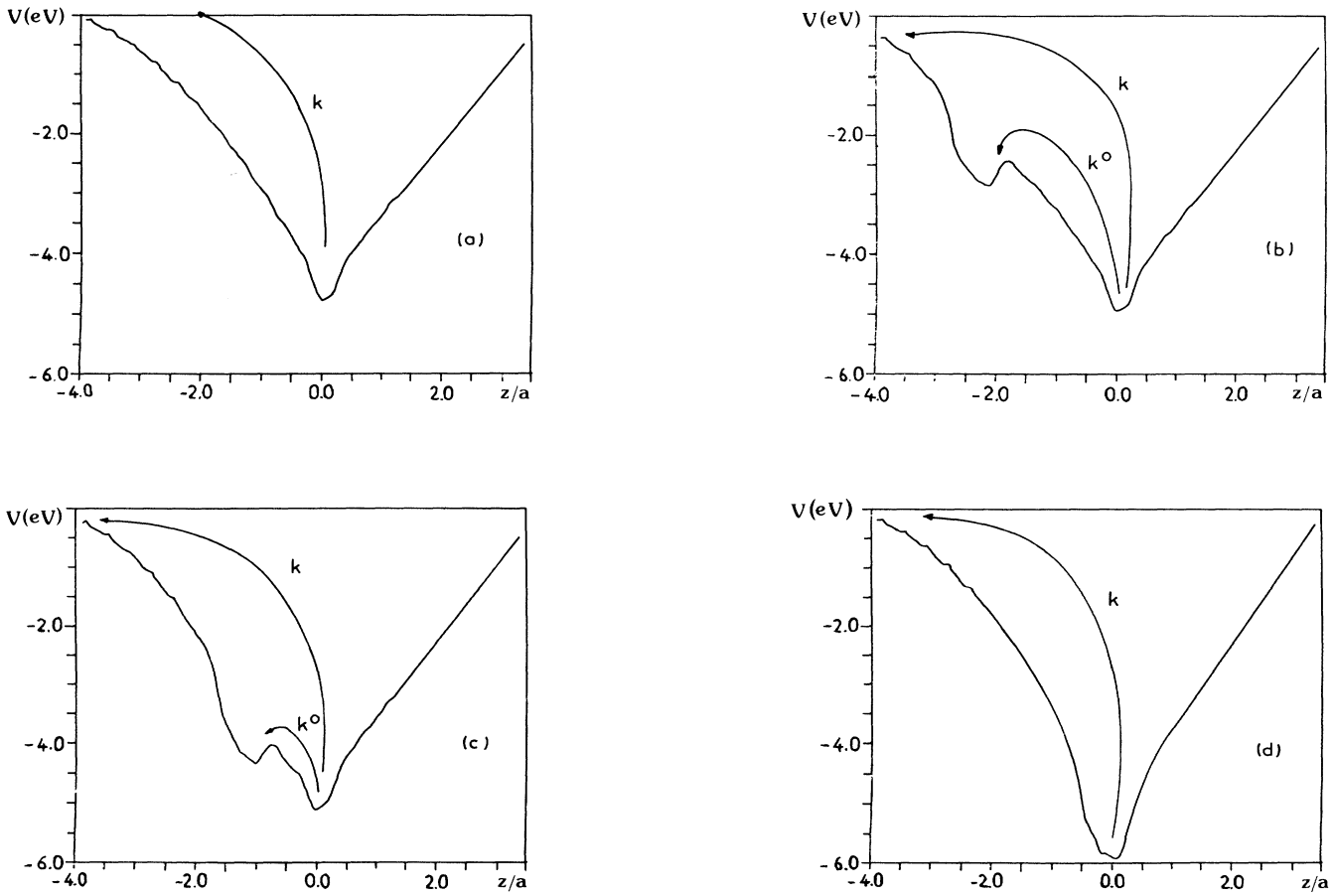

FIG. 4. Potential curves for the proton diffusion through the quartz surface; same as Fig. 2.

potential depths ΔV^0 and ΔV. The first quantity corresponds to the barrier that the various ions must overcome to penetrate the sample; the second one describes the surface influence extent, since it appears as the energy difference between the ion and the quartz crystal, with and without the surface. It may be noted that the surface influences the ion potential over a range of about 20–25 Å. The values of ΔV^0 are around a fraction of eV for Li^+, whereas they can reach 1–2 eV for Na^+ and H^+, and they significantly depend on the Al location. The ΔV values vary from 3.3 eV for Li^+ to 6.5 eV for Na^+.

The corresponding jump frequencies k^0 and k, calculated from Eq. (3), are also tabulated for the various cases considered in Figs. 2–4. Since $\Delta V^0 \leq \Delta V$, the frequency for a jump of M^+ (or H^+) from vacuum into the matter is obviously much larger than the frequency for a jump of the same ion from vacuum to the bulk crystal without surface influence. The jump frequency k (and not k^0) is the quantity that characterizes the ability for the penetration of the alkali-metal ions and of the proton into quartz.

The potential energies connected to the ion-Pt foil and to the ion-surface dipole interactions are drawn in a separate way, in Fig. 5. $V^{Pt}_{M,H}$ depends on the interface thickness between the quartz and platinum surfaces, and three cases that correspond to $D=4$, 10, and 20 Å have been studied. Within this range of the distances between the Pt foil and the M^+ (H^+) ion, the metal surface tends to attract the cation whatever its location outside or inside the crystal. In the second case, the screening effect of quartz is very serious and the repelling effect of the metal becomes inefficient. The $V^{Pt}_{M,H}$ potential has an antagonistic influence on the above potentials discussed in Figs. 2–4 and it modifies mainly the shape of these curves on the right-hand side of the figures ($z>0$) by increasing their slopes in the range $0 \leq z \leq a$.

As the macroscopic external field does not significantly influence the previous potential curves, the remaining potential, which can modify the shapes studied in Figs. 2–4, is $V_{M,\text{H-dipole}}$, also drawn in Fig. 5. This potential, calculated for an ordered dipole slab on the quartz surface with fixed orientation, is constant outside and inside the quartz crystal, with an energy difference due to the screening effect in quartz. Close to the surface, this potential decreases sharply. The values of the extrema (3 and −1.3 eV) correspond to the situation of perfectly or-

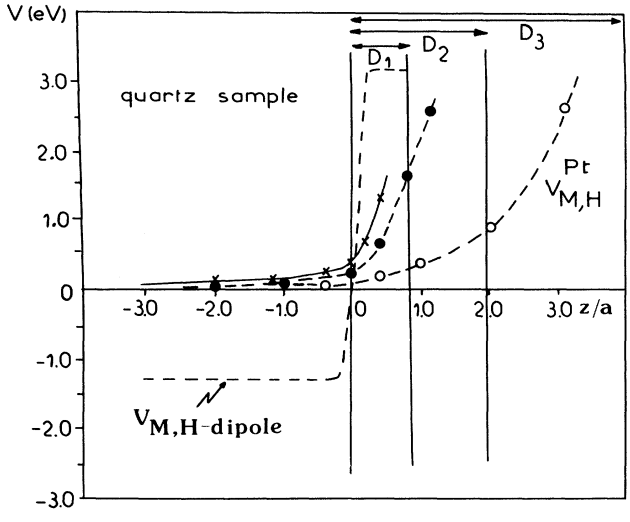

FIG. 5. Ion-metal potential $V^{Pt}_{M,H}$ for three characteristic thicknesses D of the interface (×, $D=4$ Å; ●, $D=10$ Å; and ○, $D=20$ Å); and ion-surface dipole potential $V_{M,\text{H-dipole}}$ (— — —) for a perfectly ordered and oriented dipole slab. The quartz and Pt-foil surfaces are schematized by vertical lines.

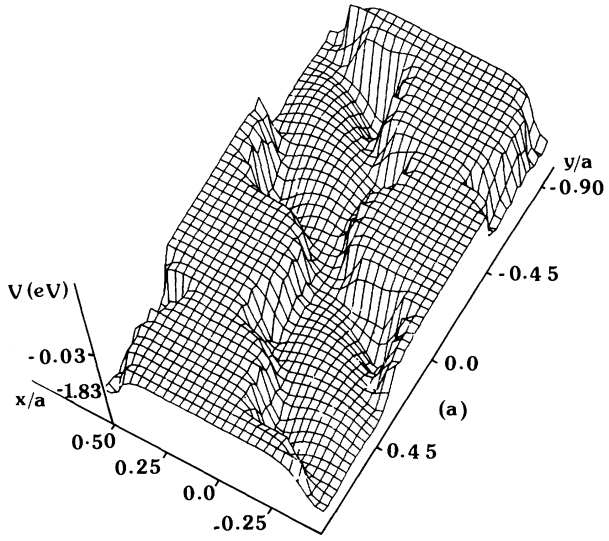

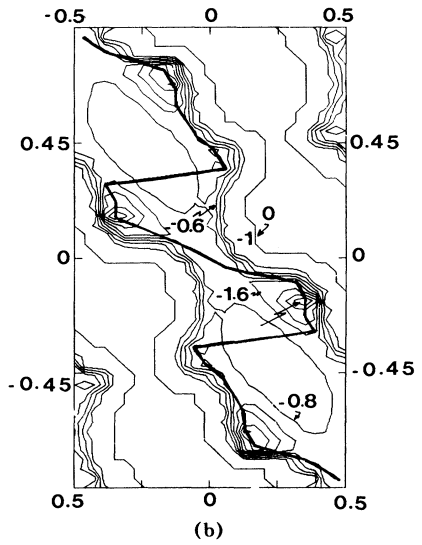

FIG. 6. Potential surface $V(x,y)$ for the superficial migration (inside the $z=0$ plane) of the Li^+ ion. (a) Three-dimensional representation, the energy origin V_0 is taken to be equal to −3 eV. All the points with $V>V_0$ have been artificially taken to have a zero energy on the map. (b) Equipotentials $V(x,y)$ and diffusion (reaction) path (——). The coordinates x and y are reduced by the cell parameter a.

dered dipole moments since the z component of μ is equal to 0.86 D. In fact, both temperature and phenomena connected to interface properties could induce a strong decrease of the potential extrema. As a result of the inclusion of this potential in the curves of Figs. 2–4, the well depths connected to the surface penetration by M^+ (H^+) ions will then be enhanced and the jump frequency will still decrease.

C. Superficial diffusion of ions

Figures 6–8 exhibit the potential energies $V(x,y)$ experienced by Li^+, Na^+, and H^+, respectively, when the centers of mass of these ions are located in the surface plane $z=0$. Only the case of a perfect optical channel, without Al center, is drawn here. The situations with a trivalent center close to the surface would give qualitatively similar shapes. In Figs. 6(a) and 7(a), the potential surfaces exhibit two regions of minima symmetrical with respect to the origin ($x=y=0$), each with two potential valleys located at the region's sides. Figures 6(b) and 7(b) illustrate better these valleys with the corresponding diffusion coordinate u in each case. The occurrence of these valleys is directly connected to the presence of the OH bonds in the surface region and to the geometry of the quartz surface.

For the proton [Figs. 8(a) and 8(b)], the shape of the potential surface looks very different, since the minimum regions become maximum regions and vice versa. This fact may be explained as a consequence of the different repulsive potentials for the alkali-metal ions and for the

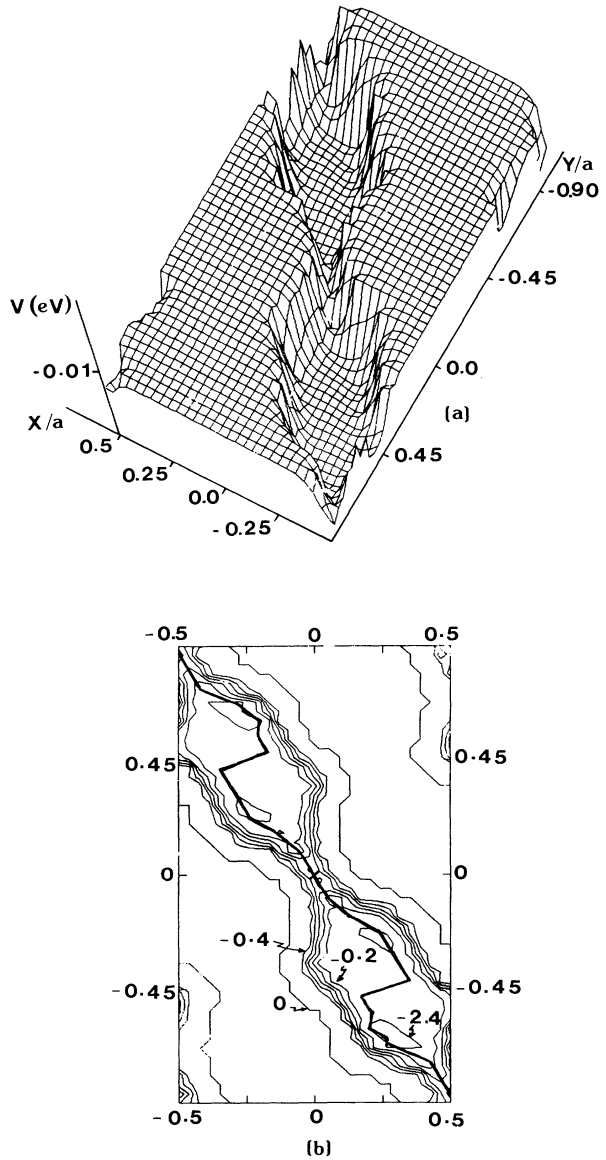

FIG. 7. Same as Fig. 6 for Na^+, $V_0=-4$ eV.

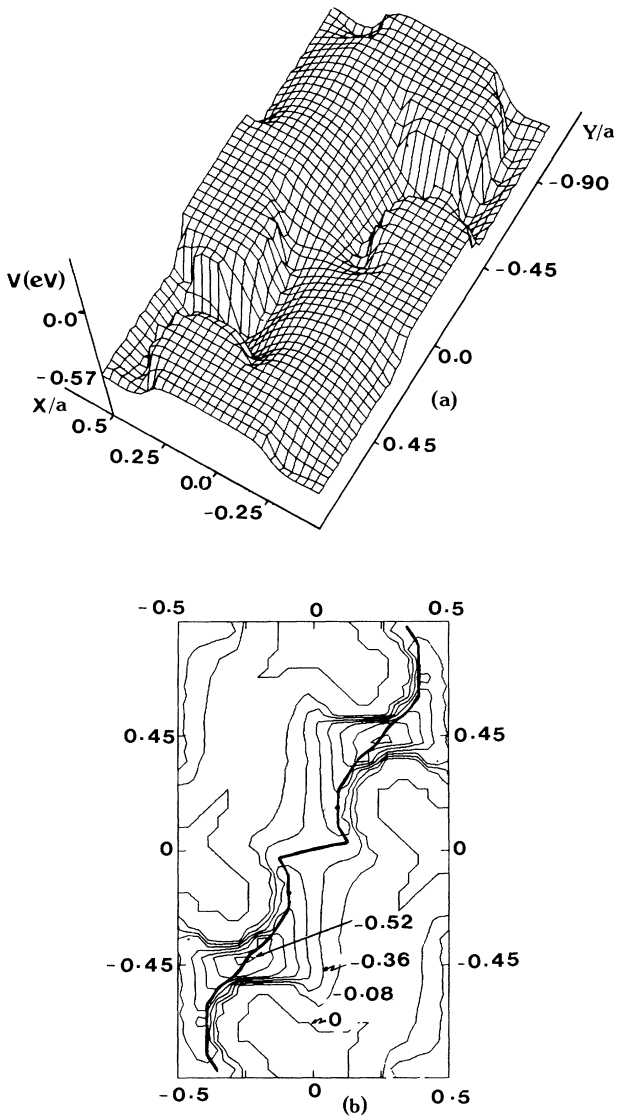

FIG. 8. Same as Fig. 6 for the proton, $V_0=-4.2$ eV.

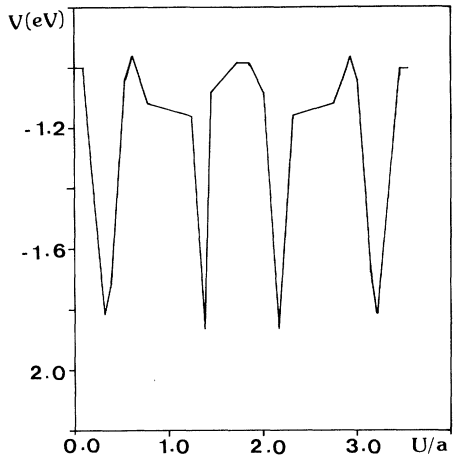

FIG. 9. Potential curve experienced by the Li^+ ion along the superficial diffusion path (Fig. 6).

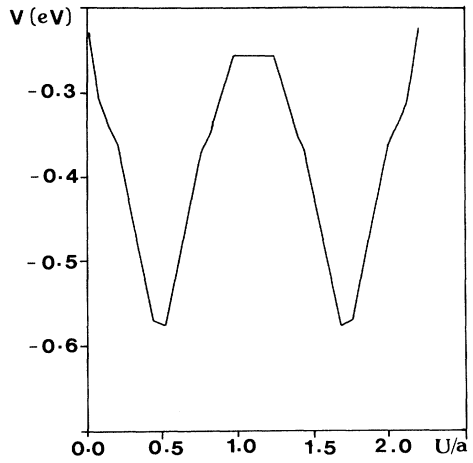

FIG. 11. Same as Fig. 9 for the proton.

proton. Moreover, the superficial diffusion path appears simpler and more direct in the valley than for the alkali-metal ions.

The potential shapes along the migration coordinate on the quartz surface are shown in Figs. 9–11 for Li^+, Na^+, and H^+, respectively. The curve for Li^+ exhibits many sharp potential wells with a depth of about 0.9 eV, whereas the wells are larger and less deep (≤ 0.6 eV) for Na^+. For the proton, two symmetrical wells with only a depth equal to 0.32 eV are calculated.

We give, in Table III, the barrier heights for the superficial migration of the ions and the corresponding jump frequencies k^s. These frequencies are much greater than the frequencies k associated with the penetration mechanism inside the quartz sample. This diffusion thus appears to be an efficient process, over short times, whereas the penetration mechanism proceeds over long times.

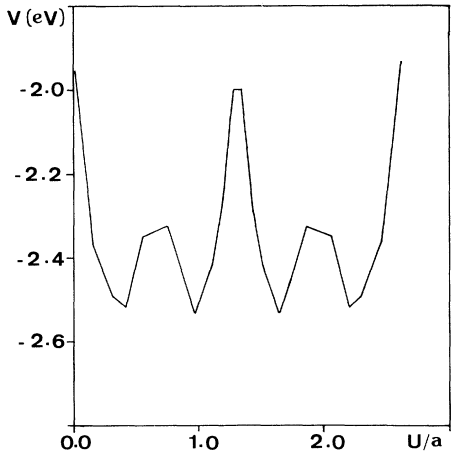

FIG. 10. Same as Fig. 9 for Na^+.

V. CONCLUSION

The present results, which are devoted to the penetration or escape mechanism of protons and of alkali-metal ions from a β-quartz crystal, can be compared to those obtained in Refs. 5 and 6, and are relative to the bulk electrodiffusion of the same species in quartz channels. It had been shown[5] that the ionic current density obtained by electrodiffusion of quartz, at $T=750$ K and for a macroscopic electric field of about 2000 V cm^{-1}, depends on three processes: the bulk diffusion in perfect channels, the trapping of ions by the trivalent impurity centers, and the surface effects. The first process had been shown to be negligible in the ionic current intensity when compared to the efficient ion trapping mechanism of the Al center. We show here that, among the two surface processes considered here, the diffusion of an ion on the surface is inefficient, whereas the penetration or escape mechanism through the quartz surface plays an essential role. Indeed, this latter mechanism is the slowest among all the others by several orders of magnitude. It will thus be as dominant a mechanism leading to the electrodiffusion current, as well as in the transient regime, as that in the steady-state regime (residual ionic current).

The model has some drawbacks; more particularly, it is semiquantitative in the sense that (i) the quartz surface is highly idealized in the model, (ii) it is a somewhat difficult task to quantify the influence of the metal foils on the ion

TABLE III. Potential depths ΔV^s (eV) for the superficial migration and jump frequencies k^s (s^{-1}) at $T=750$ K.

Ion	ΔV^s	k^s
Li^+	0.9	3.7×10^7
Na^+	0.6	3.5×10^8
H^+	0.3	3.9×10^{10}

diffusion, and (iii) the probably efficient reverse mechanism of electron penetration in the sample has been disregarded. Electromigration experiments on cleaner quartz samples with better defined surface states would stimulate more accurate theoretical approaches of this mechanism.

ACKNOWLEDGMENTS

Laboratoire de Physique Moléculaire is "Unité" associeé au Centre National de la Recherche Scientifique No. 772.

*Corresponding author.

[1]J. C. Brice, Rev. Mod. Phys. **57**, 105 (1985); J. A. Weil, Phys. Chem. Minerals **10**, 149 (1984); J. Minge, J. A. Weil, and D. G. McGavin, Phys. Rev. B **40**, 6490 (1989).

[2]L. E. Halliburton, M. E. Markes, and J. J. Martin, in *Proceedings of the 34th Annual Frequency Control Symposium,* Ft. Monmouth, New Jersey, 1980 (available from Electronic Industries Associates, 2001 I Street, N.W., Washington, DC 20006), p. 1.

[3]L. E. Halliburton, N. Koumwakalis, H. E. Markes, and J. J. Martin, J. Appl. Phys. **52**, 3565 (1981); H. Jain and A. S. Novick, *ibid.* **53**, 477 (1982); J. J. Martin, R. B. Bossoli, L. E. Halliburton, B. Subramaniam, and J. D. West, in *Proceedings of the 37th Annual Frequency Control Symposium,* Ft. Monmouth, New Jersey, 1983 (available from Electronic Industries Associates, 2001 I Street, N.W., Washington, DC 20006), p. 164, and references therein.

[4]J. Breton and C. Girardet, Phys. Rev. B **33**, 8748 (1986).

[5]J. Plata, J. Breton, and C. Girardet, Phys. Rev. B **38**, 3482 (1988).

[6]C. Girardet, J. Plata, J. Breton, and A. Hardisson, Phys. Rev. B **38**, 5648 (1988).

[7]J. Plata, J. Breton, V. Delgado, E. Alvira, and C. Girardet, Phys. Rev. B **39**, 8689 (1989).

[8]S. H. Garofalini, J. Chem. Phys. **78**, 2069 (1983).

[9]R. Bourquin (private communication).

[10]H. Schröder, J. Chem. Phys. **79**, 1991 (1983).

[11]L. Vega, J. Breton, and C. Girardet, Chem. Phys. **113**, 391 (1987).

[12]N. V. Smith, C. T. Chen, and M. Weinert, Phys. Rev. B **40**, 7565 (1989).

[13]The calculation of the potential $V_{M,\mathrm{H}}^{\mathrm{Pt}}$ [Eq. (8)] is carried out for an interface thickness which is varied from $D=4$ Å to $D=20$ Å. The surface defect and corrugation are disregarded.